Earth and Planetary Science Letters 285 (2009) 251–262

Contents lists available at ScienceDirect

Earth and Planetary Science Letters

journal homepage: www.elsevier.com/locate/epsl

Evidence for intrusive activity on Mercury from the first MESSENGER flyby

James W. Head [a,*], Scott L. Murchie [b], Louise M. Prockter [b], Sean C. Solomon [c], Robert G. Strom [d], Clark R. Chapman [e], Thomas R. Watters [f], David T. Blewett [b], J.J. Gillis-Davis [g], Caleb I. Fassett [a], James L. Dickson [a], Debra M. Hurwitz [a], Lillian R. Ostrach [a,1]

[a] Department of Geological Sciences, Brown University, Providence, RI 02912, USA
[b] Johns Hopkins University Applied Physics Laboratory, Laurel, MD 20723, USA
[c] Department of Terrestrial Magnetism, Carnegie Institution of Washington, Washington, DC 20015, USA
[d] Lunar and Planetary Laboratory, University of Arizona, Tucson, AZ 85721, USA
[e] Southwest Research Institute, 1050 Walnut Street, Boulder, CO 80302, USA
[f] Center for Earth and Planetary Studies, National Air and Space Museum, Smithsonian Institution, Washington, DC 20560, USA
[g] Hawaii Institute of Geophysics and Planetology, University of Hawaii, Honolulu, HI 96822, USA

ARTICLE INFO

Article history:
Accepted 4 March 2009
Available online 21 April 2009

Editor: T. Spohn

Keywords:
Mercury
dikes
intrusion
graben
MESSENGER

ABSTRACT

Images from MESSENGER's first flyby of Mercury have shown convincing evidence for surface volcanism. Here we report on evidence in the new data for several features that are characterized by fractures and graben — rare features on a planet dominated by contractional deformation — that may be linked to intrusive activity. These features include: (1) A floor-fractured crater, interpreted to have been the site of laccolith-like sill intrusions; the feature is similar to some floor-fractured craters on the Moon and shows evidence for individual fractured dome-like uplifts on the floor. (2) A concentric complex of graben, observed inside the peak ring on the floor of the ~250-km-diameter Raditladi basin and associated with dark plains and possibly embayed by them; the feature may represent an unusual type of floor-fracturing associated with deeper intrusions and related ring dikes or cone sheets, or the graben may instead be the product of non-magmatic uplift of the basin floor. (3) A large radial graben swarm, Pantheon Fossae, located near the center of the Caloris basin, thus far unique on Mercury, and characterized by hundreds of individual graben segments ranging from ~5 km to ~110 km in length. In the nexus, graben crosscut one another and produce a local polygonal pattern; others curve away from the center as the nexus is approached. Two scales of graben length are observed; the radius of the dense radially symmetric plexus of graben is ~175 km, and a few graben extend to greater radial distances to the north and southwest out to distances that intersect with a ring of generally concentric graben around the outer basin floor. Two width scales of graben are observed; a large graben about 8 km wide emerges from the nexus and extends for ~100 km; most graben are less than half this width. Some graben walls appear cuspate, with convex-outward wall segments that resemble crater chain segments. One crater chain with distinctive raised rims parallels nearby graben. Locally, some graben appear in *en echelon* patterns, and smaller graben sometimes show cross-cutting (superposition) relationships. Abundant impact craters, the most prominent being Apollodorus, and secondary crater clusters and chains are superposed on the graben system; there is little evidence that craters greater than 5 km in diameter have been cut by a graben. This relation implies that the graben swarm formed soon after the emplacement of the Caloris floor plains. These graben are interpreted to be the surface expression of a radial dike swarm emanating from a subsurface magma reservoir. Similar features, in which the dikes contribute to a near-surface stress field that favors radial graben, are known on the Earth, Venus, and Mars. The location of Pantheon Fossae in the center of the Caloris basin suggests that formation of the radial graben structure is linked to basin evolution.

1. Introduction and background

Magmatism is the process of emplacement and solidification of igneous rock from molten material (magma) derived from a planetary interior. It is commonly subdivided into plutonic or intrusive processes, which involve magma movement and solidification in the subsurface, and volcanic or extrusive processes, which involve

* Corresponding author.
E-mail address: James_Head@brown.edu (J.W. Head).
[1] Now at: School of Earth and Space Exploration, Arizona State University, Tempe, AZ 85287 USA.

0012-821X/$ – see front matter © 2009 Elsevier B.V. All rights reserved.
doi:10.1016/j.epsl.2009.03.008

eruption onto the surface and emplacement and solidification of magma as effusive lava flows or explosive tephra. The first flyby of Mercury by the MErcury Surface, Space ENvironment, GEochemistry, and Ranging (MESSENGER) spacecraft on 14 January 2008 obtained images of 21% of the surface not seen by the Mariner 10 spacecraft (Solomon et al., 2008), including the remainder of the Caloris basin and new regions near the terminator showing details of the nature of smooth and intercrater plains. Images from MESSENGER's Mercury Dual Imaging System (MDIS) have helped to address and resolve a series of questions related to the existence, nature, and distribution of magmatism (volcanism and plutonism) that have been largely outstanding since the end of the Mariner 10 mission in 1975. In separate contributions, we have outlined the evidence that supports and confirms earlier hypotheses from Mariner 10 data that volcanism was important in shaping the surface of Mercury; this new evidence includes the presence of volcanic vents, a shield-like structure, spectrally distinct plains embaying adjacent units, and spectrally distinct mantling deposits interpreted to be of pyroclastic origin (Head et al., 2008; Robinson et al., 2008; Murchie et al., 2008; Blewett et al., 2009-this issue; Kerber et al., 2009-this issue; Head et al., 2009-this issue). In this contribution we assess the evidence for the surface manifestation of intrusive magmatic activity on the basis of the MDIS images obtained during the first flyby.

Magma reaches the surface through propagating magma-filled cracks (dikes), its rise driven by overburden pressures, magma overpressure, and thermal and chemical buoyancy variations (Fig. 1). On the Moon, where dikes propagate from great depths and eruptions were infrequent even during the peak of mare volcanism, eruptions tend to be characterized by high rates of ascent and eruption (Head and Wilson, 1992). Shallow magma reservoirs, commonly formed by multiple dike intrusions at a zone of neutral buoyancy, are uncommon (Head and Wilson, 1991). Moderate- to large-diameter volcanic edifices, built from multiple phases of inflation, lateral and vertical dike emplacement events, and eruptions from shallow magma reservoirs, are not observed on the Moon (Head and Wilson, 1991) but are common on the Earth, Venus, and Mars (Head et al., 1992; Carr, 2006). Mercury, like the Moon, is dominated by extensive plains units, a few visible volcanic vents, but (as yet) no major volcanic edifices on the scale of the Tharsis Montes on Mars (Head et al., 2008, 2009-this issue), a style and surface character typical of small one-plate planetary bodies for which the lithosphere thickened comparatively rapidly early in the planet's history (Solomon, 1977, 1978). On the Moon, the surface manifestation of intrusive magmatic activity is found in graben, often marking the presence of dikes intruding to near the surface, and their associated features (Fig. 1) (Head and Wilson, 1993), and in floor-fractured craters, interpreted to be the surface manifestation of sill formation beneath crater floors (Schultz, 1976). Here we examine occurrences of such features in impact craters and basins on Mercury documented in MDIS images, and we explore the implications of these occurrences for the presence and significance of plutonic activity on the innermost planet.

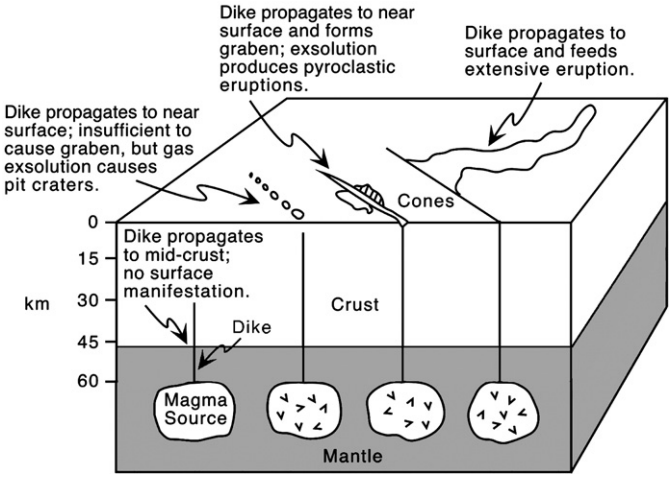

Fig. 1. Relationship of dikes to their surface environment, showing several different manifestation of dikes as they propagate from mantle magma reservoirs into the crust, approach the surface, and stall or erupt. After Wilson and Head (2008).

2. Floor-fractured craters

Despite the paucity of shallow magma reservoirs on the Moon, there is evidence for local sill formation, caused by lateral intrusion of magma from vertically propagating dikes at density or material–property boundaries to create horizontal lenses of magma in the shallow crust. The most compelling evidence for shallow sill formation is the presence of floor-fractured craters, impact craters whose floors have been fractured, uplifted, and often partially flooded by lava flows (Schultz, 1976) (Fig. 2). Dikes intruding into the shallow crust are interpreted to have formed sill-like bodies preferentially along the base of the low-density brecciated zone in the crater interior. On the Moon, floor-fractured craters occur predominantly along the margins of the lunar mare basins. Such craters often have moats around the uplifted interior floor. Other associated features include dark-halo craters located along the floor fractures, the most well-known example of which is the crater Alphonsus (Head and Wilson, 1979). Schultz (1976) identified seven different classes of floor-fractured craters on the Moon, related to both the initial geometry of the crater and to the stages in the evolution of its modification. An alternative explanation for floor fracturing is viscous or viscoelastic relaxation of topographic relief, enhanced by higher than normal subsurface temperatures in the vicinity of impact basins (Hall et al., 1981). The most detailed models of such a mechanism, however, cannot account for floor uplift and fracturing for craters smaller than about 100 km in diameter (Dombard and Gillis, 2001).

Although Mariner 10 image resolution and illumination geometries were not the most favorable for detection and documentation of floor-fractured craters on Mercury, Schultz (1977) reviewed candidate examples of endogenic modification of impact craters on Mercury and found evidence for crater floor units and structures of possible volcanic origin, as well as for uplift and possible fracturing. MESSENGER's first Mercury flyby revealed a single example of a classic lunar-like floor-fractured crater (Figs. 3 and 4) in the vicinity of the terminator; although for MESSENGER, too, the illumination geometry was less than favorable for the detection of floor-fractured craters over much of the rest of the area imaged. This ~35-km-diameter floor-fractured crater (Fig. 3B), briefly described by Head et al. (2008), is located near the margins of extensive deposits of smooth and intercrater plains that have been interpreted to be of volcanic origin by Robinson et al. (2008) and Head et al. (2009-this issue) (compare with the perspective view of Gassendi, Fig. 2 top and lower left). Relatively fresh impact craters of comparable size are characterized by raised rims, terraced walls, flat floors, and central peaks (Pike, 1988) (Fig. 3B). In contrast, the interior of this crater (Fig. 3B, C) appears highly modified, with the south–southeastern wall slumped inward, wall terraces indistinct and obscured, and the floor of the crater generally appearing shallower than for the fresh example. The exterior of the crater is clearly embayed on its western margins by smooth plains (Fig. 3B, C).

Although no concentric fractures and moats typical of large lunar floor-fractured craters are seen, the most distinctive parts of the crater interior are two dome-like or plateau-like features located on the eastern and western parts of the crater floor. These dome-like features are unlike central peaks in their morphology and position (compare Fig. 3B, C with Fig. 3A). Peak rings form mountains and hummocks surrounding the crater center but do not occur in fresh craters of this size (Pike, 1988) and are morphologically dissimilar to these features

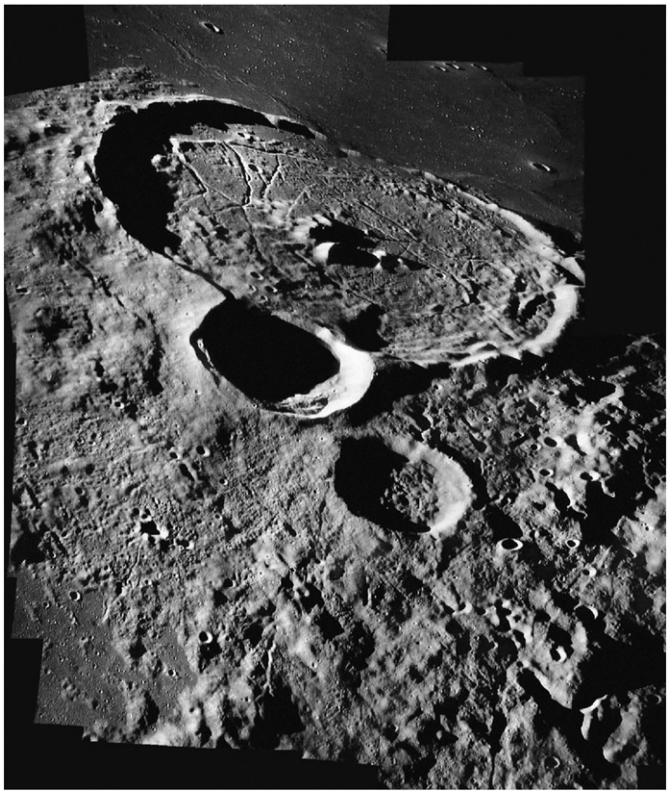

Fig. 2. Oblique view from the north of the lunar floor-fractured crater Gassendi, 110 km in diameter. Note the shallow floor, the multiple floor fractures, and the lavas that flooded the southern part of the crater from Mare Humorum to the south. The central peaks rise higher than portions of the rim crest. Mosaic of Apollo 16 images AS16-120-19278 through AS16-120-19313.

(compare Figs. 3B and 5A). The western dome-like feature is irregularly shaped, about 12 km by 17 km, and contains a network of fractures each less than about 1 km in width on its summit and southern part. The eastern dome-like feature is also irregularly shaped, about 9 km by 15 km, and contains less well-developed fractures on its southeastern flank. In lunar floor-fractured craters, as exemplified by the larger crater Gassendi (Fig. 2), the uplift of the entire flat crater floor (and central peak), the creation of a moat outward of the uplifted central floor (Fig. 4A), and the flooding of the moat are the evidence that supports the interpretation of a shallow intrusion and inflation of a broad sill-like structure. For the crater on Mercury (Fig. 3B, C), however, in addition to more moderate floor uplift than for Gassendi, floor modification appears more localized and focused at these two dome-like locations.

This floor-fractured crater appears to be most similar to lunar Class IVB of Schultz (1976), as exemplified by the lunar crater Gaudibert, at 33-km diameter a crater comparable in size to the crater on Mercury, located along the northeastern edge of Mare Nectaris (10.9°S, 37.8°E) (Fig. 4). Class IV lunar floor-fractured craters are shallow and characterized by a narrow floor moat (usually v-shaped in cross-sectional profile) adjacent to the inner wall. The interior border of the moat is often ridge-like, and in Gaudibert (Fig. 4) the border is in places at a higher elevation than the rim (Schultz, 1976) (compare Figs. 3B and 4A). Schultz (1976) interpreted the differences between Class III (e.g., Gasssendi, Fig. 2) and Class IV (e.g., Gaudibert, Fig. 4) lunar floor-fractured craters to be to the result of differences in the size of the initial crater and its corresponding morphology (greater development of wall terraces and greater expanse of flat floor in larger craters; Pike, 1980), and he introduced cross-sectional interpretations of sill emplacement and floor fracturing that were similar in process but differed in detail (compare his Figs. 10 and 15).

Gaudibert also shows interior dome-like features, and there are hints of the presence of associated fractures (Fig. 4A). Furthermore, Gaudibert occurs along the margin of Mare Nectaris, and Clementine images (Fig. 4) show the proximity of the low-albedo mare deposits and the occurrence of low-albedo material on the southern floor of the Gaudibert crater, in association with a rimless depression of possible volcanic origin. The Mercury example (Fig. 3A) occurs along the margin of smooth plains interpreted to be of volcanic origin (Head et al., 2008, 2009-this issue). On the basis of these associations and characteristics, we interpret the features in the Mercury crater to be the result of local sill-like intrusions, following the general interpretations of Schultz (1976) for lunar craters, but in the Mercury case (and perhaps in Gaudibert) we interpret the sills to have a more laccolith-like structure, where the central part of the sill inflates, upbowing and fracturing the overlying substrate (Figs. 3B, C and 4A). Rimless depressions on crater floors on Mercury, detected in MESSENGER images, have also been interpreted as evidence of near-surface magmatic activity (Gillis-Davis et al., 2009-this issue), although they are not associated with extensive floor-fracturing.

The global distribution of floor-fractured craters on Mercury is currently unknown. As pointed out by Schultz (1977), the illumination geometry is critical to detection of floor-fractured craters, with shallow crater topography and detailed tectonic structure much more obvious at low Sun elevation angles than at high. The detection

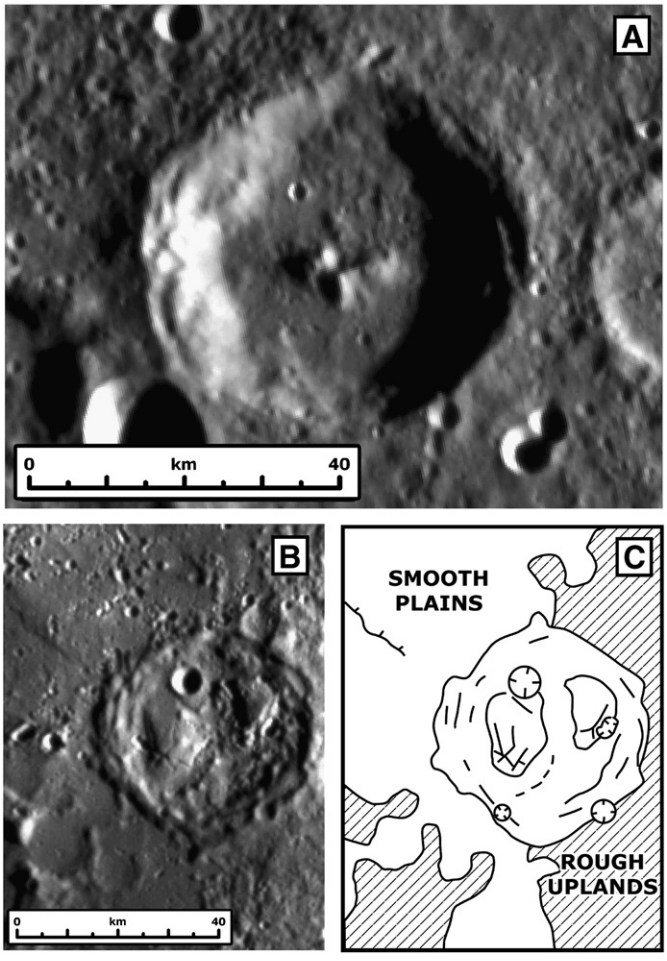

Fig. 3. Relatively fresh crater on Mercury compared with a floor-fractured crater observed during the first MESSENGER flyby. (A) Typical relatively fresh impact crater about 49 km in diameter on Mercury (24.3°N, 105.4°E). MDIS narrow-angle camera (NAC) image EN0108826782M. (B) Floor-fractured ~35-km-diameter crater on Mercury (7.5°N, 104.3°E) (see Head et al., 2008). MDIS NAC image EN0108826977M. (C) Sketch map of major features in (B) showing domes and fractures and proximity to smooth plains.

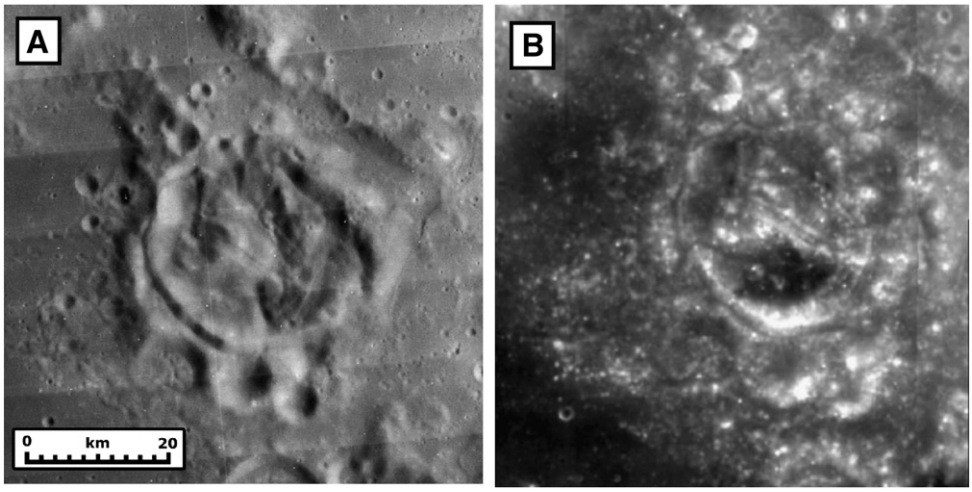

Fig. 4. Gaudibert floor-fractured crater on the Moon, ~33 km in diameter. (A) Lunar Orbiter 4 image (LO-IV-072H); illumination geometry emphasizes morphology. (B) Clementine image; illumination geometry emphasizes albedo differences. Compare floor-fractured craters on the Moon (Fig. 4A) and Mercury (Fig. 3B).

near the terminator (optimal illumination conditions) of one floor-fractured crater in images from the first MESSENGER flyby suggests that others may be detected under more favorable illumination conditions. As yet, however, no large, complex, floor-fractured craters such as the lunar crater Gassendi (Fig. 2) have been observed on Mercury. The general global contractional tectonic environment (Solomon et al., 2008) may mean that shallow crustal stress environments and principal stress orientations favoring shallow sill-like intrusions may have been less common on Mercury than on the Moon. Global image and altimetry coverage provided by future MESSENGER and BepiColombo (Benkhoff et al., in press) mission operations will help to address these questions.

3. Concentric graben on the floor of Raditladi basin

MESSENGER images also revealed fractures and graben on the floor of the ~250-km-diameter Raditladi basin (Fig. 5) (see also Prockter et al., 2008; Watters et al., 2009b-this issue). Unlike typically broad patterns of floor fractures on the Moon (Schultz, 1976), as exemplified by the 110-diameter crater Gassendi (Fig. 2), the floor fracturing in Raditladi is focused within the inner ring and consists of a series of narrow concentric graben structures with no direct evidence at current resolution for an unusually shallow crater floor or associated vents or dark-halo craters. Two small, elongated craters that may be volcanic vents are seen on the northern part of the crater floor (Fig. 5B, C). The peak ring is offset to the northwest from the center of the crater defined by the crater rim crest. The center of the ring of graben, however, is located close to the center of the crater defined by the crater rim crest and is offset toward the southeast from the center of the peak ring.

One possible interpretation is that a sill-like intrusion and related floor fracturing were limited to a zone within the basin peak ring, rather than spread across the entire crater floor as is the case in Gassendi (Fig. 2) or the lunar crater Taruntius (Wichman and Schultz, 1996). If this is the case, any uplift would have to be very limited, as the graben do not show the asymmetry (interior sides of graben higher than exterior sides) that are usually seen in marginal graben in shallow lunar floor-fractured craters such as Taruntius and Gassendi. On the basis of terrestrial crater structure, Schultz (1976) and Wichman and Schultz (1996) considered the base of the floor breccia lens to be a likely candidate for the density-contrast horizon at which sills intrude in lunar craters. The distribution of breccia lenses may be quite different in complex craters than larger peak-ring basins. For example, the breccia lens might be interrupted by the peak ring, or deeper in the peak-ring interior, and this geometry might cause intrusion of sills to be manifested differently in peak-ring basins.

Another possible interpretation for the graben structure is that it represents the surface manifestation of magmatic intrusions known as ring dikes or cone sheets (e.g., Schirnick et al., 1999). Ring dikes on Earth consist of one or more sets of concentric fracture systems along which lavas intrude and surface volcanic features often form. Ring dikes form a magma-filled cylinder around a block of country rock. Cone sheets are thin intrusive sheets a few meters thick that expand upwards and outwards in cones and converge towards a common source at depth, usually a magma reservoir. Ring dikes and cone sheets often occur together, as exemplified by the classic examples on the islands of Mull and Skye, Scotland. Anderson (1936) studied the dynamics of formation of cone sheets and ring dikes, showed how displacements due to a point dilation are modified when the point is near a planar free surface, and treated the case for strain associated with the “point push.” Specifically, an upward point push at a specific depth could lead to the formation of cone sheets, while a downward point push at a corresponding depth could lead to the formation of ring dikes (Anderson, 1936). More recent analyses (Le Bas, 1971; Phillips, 1974) have explored the geology and dynamics of emplacement of ring dikes and cone sheets in terrestrial environments. Most ring dikes and cone sheets on Earth are exposed by hundreds of meters of erosion, and thus the surface manifestation of these features in a fresh unweathered environment is not known. However, on the basis of the dynamics of intrusion (Anderson, 1936; Le Bas, 1971; Phillips, 1974), it is likely that near-surface intrusions of both cone sheets and ring dikes would result in concentric graben. Thus, a possible interpretation of the concentric graben on the floor of the Raditladi basin is that they represent the surface manifestation of ring dikes and/or cone sheets, forming above a magma reservoir. This configuration would differ in geometry from the traditional sill formation thought to be responsible for lunar floor-fractured craters (e.g., Schultz, 1976).

The Raditladi crater floor graben could also be related to late-stage tectonic modification and uplift of the basin floor (Watters et al., 2009a,b-this issue), rather than to a sill or a magma reservoir and ring dikes/cone sheets. Detailed models have not yet been developed for any of these processes in the Raditladi basin. Any hypothesis should explain the slight off-center location of the peak ring (relative to the basin rim crest), the central location of the concentric graben structure (Fig. 5) (compared with the basin rim crest), and the floor plains of presumed volcanic origin (Watters et al., 2009a,b-this issue).

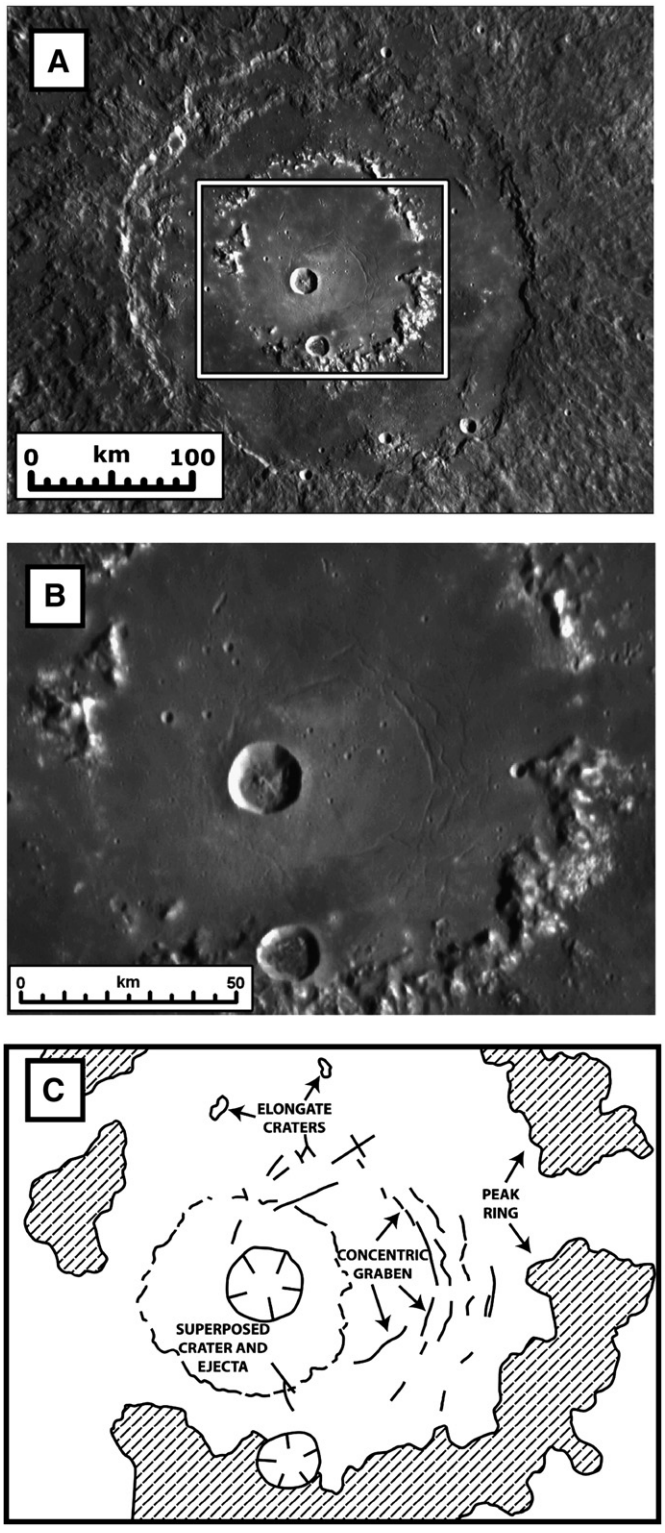

Fig. 5. The Raditladi basin, ~250 km in diameter. (A) This NAC image mosaic of the basin shows the central peak ring and floor. Mosaic of MDIS NAC images EN0108826722M, EN0108826727M, EN0108826732M, EN0108826787M, EN0108826792M, and EN0108826797M. (B) This close-up (see box in A) shows the generally concentric graben structures, centered on the crater center defined by the rim crest, but slightly offset to the southeast from the center of the peak ring. Mosaic of MDIS NAC images EN0108826727M and EN0108826792M. (C) Sketch map of area in (B), showing the peak ring, the generally concentric graben system, the large superposed impact crater, and two elongate craters that may be vents for the dark material on the crater floor.

New MESSENGER data such as altimetry of the Raditladi basin as well as the search for other similar basins elsewhere on Mercury will help in formulating and constraining such models.

4. Radial graben swarm: Pantheon Fossae

One of the most striking features observed in images from MESSENGER's first Mercury flyby is the radial graben structure Pantheon Fossae, centered in the Caloris basin (Figs. 6–8) (Head et al., 2008; Murchie et al., 2008; Watters et al., 2009a-this issue). Its location central to the Caloris basin interior, its numerous graben radiating away from a nexus, or central core, and its geographic association with Apollodorus crater have led to a range of hypotheses for its origin. These include: (1) uplift and radial fracturing of the center of Caloris following volcanic infill of the basin floor (Murchie et al., 2008; Watters et al., 2009a,b-this issue); (2) stress release and fracturing triggered by the Apollodorus impact (Freed et al., 2009-this issue); and (3) radial dike emplacement from a shallow magma reservoir (Head et al., 2008). Here we further explore the radial dike emplacement interpretation and the possibility that these features might mark the presence of a magma reservoir in the center of the Caloris basin (Fig. 6).

As described by Murchie et al. (2008), Head et al. (2008), and Watters et al. (2009a,b-this issue), the Pantheon Fossae complex is centrally located in the Caloris basin and consists of over 230 linear troughs or graben that radiate away from a common center (Fig. 7). Detailed analysis of individual portions of Pantheon Fossae reveals the following characteristics:

(1) *General characteristics of graben*: The lengths of individual graben segments range from ~5 km up to ~110 km, and widths range from 1 to 8 km.
(2) *Central arcuate and polygonal patterns*: In the nexus, troughs (graben) crosscut one another and produce a local polygonal pattern (Figs. 7 and 8A). Others curve away from the center as the nexus is approached (Fig. 8H, upper left).
(3) *Two populations of graben length*: The radius of the dense radially symmetric plexus of graben is ~175 km, and a few graben extend to greater radial distances to the north and southwest (Fig. 7A–C), out to distances that intersect with a ring of generally concentric graben around the outer basin floor.
(4) *Two scales of graben width*: In the central region, just south of Apollodorus crater (Figs. 7 and 8A), a large graben about 8 km wide emerges from beneath Apollodorus crater ejecta, extends radially away from the central region for about 35 km, changes strike for about 20 km, and then again changes strike, extending about 45 km before becoming obscured beneath a superposed impact crater (Fig. 7). Toward the nexus, the width is more than twice that of the smaller graben population. The large graben decreases in width radially from the nexus; this feature appears to crosscut smaller radial graben. Two additional larger features that could be large troughs radiate to the northwest and to the southeast (Figs. 7A and 8C, H).
(5) *Cuspate walls and crater-chain-like structures*: Some of the graben walls appear cuspate, with convex-outward wall segments that resemble crater chain segments (Fig. 8B, E–G). Similar pits and chains are often seen associated with graben on the Moon and Mars. One crater chain with distinctive raised rims parallels nearby graben (Fig. 8F, lower center).
(6) *En echelon graben*: Locally, some graben appear in *en echelon* patterns (Fig. 8D, center).
(7) *Superposed (cross-cutting) graben*: In addition to the large graben mentioned above, smaller graben sometimes show cross-cutting (superposition) relationships (Fig. 8E, center; H).
(8) *Possibly embayed graben*: The laterally discontinuous nature of many graben (Fig. 8D), and the manner in which the graben

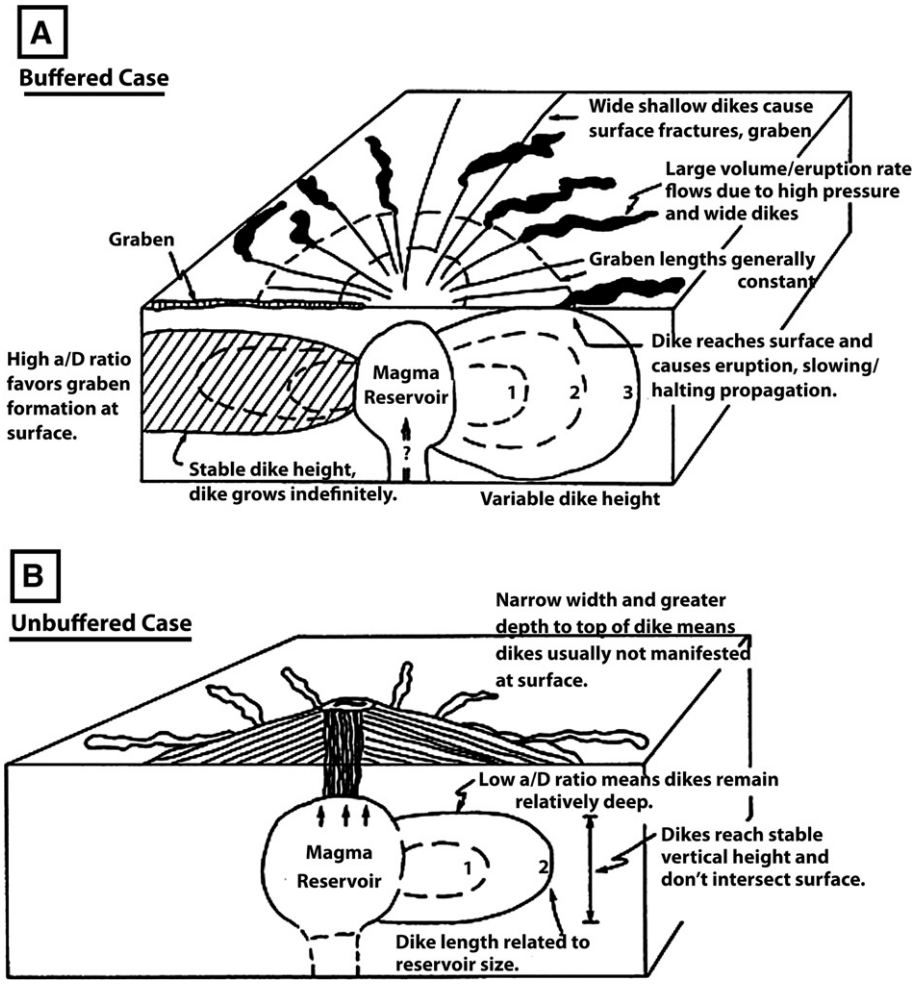

Fig. 6. Block diagrams and cross sections illustrating dike swarms and surface structure radiating away from the central region above an intrusion. (A) Schematic illustration of the behavior of dikes emplaced under buffered conditions. Depth to dike center is *D*; *a* is dike half width. (B) Schematic illustration of the behavior of dikes emplaced under unbuffered conditions. From Parfitt and Head (1993).

segments fade into the background plains at their ends (Fig. 8E, G), suggest that some of the graben may be flooded and embayed; the albedo and spectral homogeneity of the plains, however, makes definitive assessment difficult.

(9) *Superposed impact craters*: Abundant impact craters, the most prominent being Apollodorus (Figs. 7 and 8B), and secondary crater clusters and chains (Fig. 8H) are superposed on the graben system. With the possible exception of one crater (Fig. 8B, bottom center) we found no evidence of a crater greater than 5 km cut by a graben. This pattern implies that the graben swarm formed soon after the emplacement of the Caloris floor plains (Strom et al., 2008). This inference is confirmed by crater counts in a 10^5 km^2 area centered on Pantheon Fossae, which show no substantial differences from crater counts for the entire floor of Caloris presented in Strom et al. (2008).

These observations of the nature of the Pantheon Fossae complex form the basis for understanding its origin, location, and timing, and its relationship to Caloris basin fill and Apollodorus crater. Graben structures radiating away from a central rise at all scales are common occurrences on terrestrial planets and have been related at the small scale to laccolithic sill intrusions, domical uplift, and fracturing, and at the large scales to broad thermal and mechanical uplift often associated with sites of mantle upwelling (e.g., Tharsis on Mars, Banerdt et al., 1992; Beta Regio on Venus, Basilevsky and Head, 2007). At intermediate scales, such as that of Pantheon Fossae, graben commonly radiate away from volcanic edifices and subsurface magma reservoirs and are formed as the surface manifestation of radial dike emplacement (e.g., Johnson, 1961; Parfitt and Head, 1993; Ernst et al., 1995). Overpressurized shallow magma reservoirs propagate magma-filled cracks (dikes) radially away from the reservoir (Odé, 1957; Pollard and Muller, 1976; Delaney and Pollard, 1981; Gudmundsson, 1984; but see Grosfils, 2007). In cross section, these dikes appear as elongated blade-like forms (Fig. 6), and as they approach the surface they create a near-surface extensional stress field that commonly results in a graben, the width of which is related to the width of the dike and its orientation relative to the regional stress field (Pollard, 1987; Delaney, 1987; Mastin and Pollard, 1988; Parker et al., 1990) (Fig. 6A). For an isolated dike, the dike width is proportional to the total surface extension perpendicular to the dike, although the proportionality depends on other properties of the dike (Mastin and Pollard, 1988; Head and Wilson, 1993). Dikes associated with terrestrial mafic dike swarms are typically 30–50 m wide and can range up to 100–200 m in width (Ernst et al., 1995). Single dikes hundreds of meters in width are inferred for many planetary examples (Head and Wilson, 1993; Wilson and Head, 2002); multiple dike emplacement events can enlarge a graben. The resulting graben can be either laterally continuous, discontinuous, or *en echelon*, depending on the depth of the reservoir, the magnitude of the overpressurization event, modulations in the overpressurization event(s), surface topography and geology, and variations in the near-surface stress field. These same factors help determine whether a dike reaches the surface and results in eruption of lava (Pollard et al., 1983; Rubin and Pollard, 1987; Rubin, 1992). The full

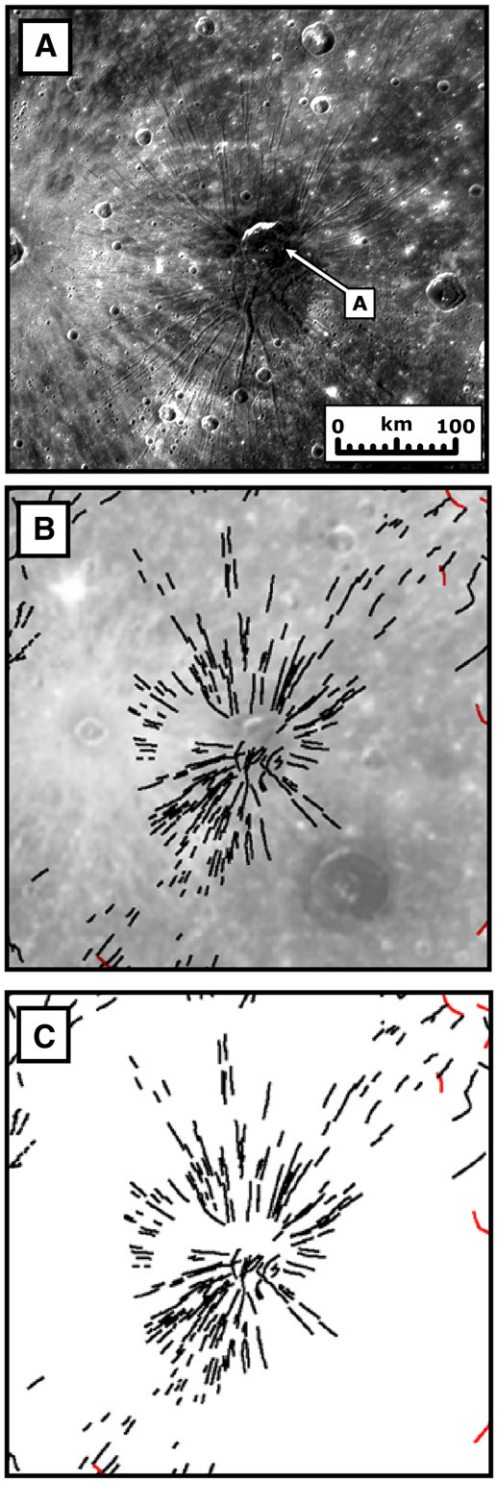

Fig. 7. Radial graben structure of Pantheon Fossae. (A) Graben (fossae) radiating from the center of the structure. Apollodorus crater (identified by the letter "A") is offset slightly to the north–northeast from that center. Mosaic of MDIS NAC images EN0108826752M, EN0108826757M, EN0108826762M, EN0108826817M, EN0108826822M, and EN01088268247M. (B) Distribution of tectonic structures in the Caloris basin with MDIS mosaic as background. Black, graben; red, wrinkle ridges (structural features interpreted to be caused by horizontal shortening). Mosaic of MDIS NAC images EN0108826752M, EN0108826757M, EN0108826762M, EN0108826817M, EN0108826822M, and EN01088268247M. (C) Structures only. (B) and (C) are from Watters et al. (2009a-in this issue); Lambert conformal projection.

range of cases (eruption dominated, mixed eruption and graben formation, only graben formation) has been observed on the terrestrial planets.

Whether the dikes propagate radially away from the reservoir, or are concentrated in discrete zones, is known to be linked to the nature of the local and regional stress field. For example, dikes propagating away from the Kilauea magma reservoir on Hawaii are concentrated in discrete rift zones, the orientation of which is controlled by the regional stresses associated with the collapse of the margins of the edifice and the formation of listric faults (Fornari, 1987; Ryan, 1988). This relationship has been used to reconstruct regional stress fields in the geological record on Earth (e.g., Johnson, 1961; Halls, 1982; Sigurdsson, 1987), Venus (Grosfils and Head, 1994a,b; Crumpler and Aubele, 2000), and Mars (Banerdt et al., 1992). Examples of radially symmetrical dikes and graben are also known (e.g., Krassilnikov and Head, 2003; Ernst et al., 2003); these occurrences imply a regionally homogeneous stress field. In these cases, individual magma-reservoir overpressurization events are not sensing a regionally heterogeneous stress field but are more likely controlled by local heterogeneities in the walls of the reservoir and thus are more random (Parfitt, 1991). Radial dike swarms propagating from magma reservoirs have also been used extensively to reconstruct widely dispersed Archaean continental fragments on Earth (Bleeker, 2002, 2003, 2004; Bleeker and Ernst, 2006).

Radial dike swarms often show two populations in terms of length, which can be understood in the context of buffered and unbuffered conditions in the magma reservoir (Parfitt and Head, 1993; Fig. 6). One population, the most abundant, is concentrated in the vicinity of the reservoir. Typical magmatic additions to the reservoir from depth, or changes within the reservoir, cause reservoir inflation, resulting in elastic expansion of the region around the reservoir. Inflation continues until the elastic expansion can no longer accommodate the increased magma supply (estimated to be less than a few percent of the reservoir volume; Blake, 1981), and at that point, brittle failure of the reservoir wall occurs and a magma-filled crack is propagated radially away from the reservoir. This situation is known as unbuffered dike emplacement from a magma reservoir (Fig. 6B) (Parfitt and Head, 1993); the magma input, inflation, and output (dike emplacement) are all relatively in equilibrium, and this pattern results in the emplacement of dikes of generally comparable length, creating the near-field dike swarm.

Occasionally, however, magma supply from depth far exceeds the norm, and the magma reservoir is no longer in equilibrium. In this situation, known as the buffered dike emplacement case (Fig. 6A) (Parfitt and Head, 1993), magma enters the reservoir and causes inflation, but once brittle failure of the reservoir wall is initiated the dike continues to propagate until the anomalous magma supply is depleted or the reservoir stresses are equilibrated. In theory, buffered magma-reservoir supply events can result in dikes radiating many multiples of the distance reached by the unbuffered dikes, up to hundreds to even thousands of kilometers away from the reservoir (Parfitt and Head, 1993), and indeed examples of these types of events are known on Hawaii (e.g., Holcomb, 1987) and the Canadian shield (Ernst and Baragar, 1992) and inferred on Mars (Wilson and Head, 2002) and Venus (Parfitt and Head, 1993; Grosfils and Head, 1994a,b; Krassilnikov and Head, 2003; Ernst et al., 2003).

These processes and the relationships observed on the terrestrial planets can be used to assess whether the Pantheon Fossae feature is a candidate for radial dike emplacement events, and if so, what its presence, characteristics, and relationships might tell us about the evolution of the Caloris basin interior. First, the size of the individual Pantheon Fossae graben and their geometry are very similar to dozens of examples of novae on Venus, interpreted to represent the surface manifestations of radial dike swarms (Krassilnikov and Head, 2003) (Fig. 9A). The radial symmetry is also similar to many of the novae seen on Venus (Krassilnikov and Head, 2003) (Fig. 9), although

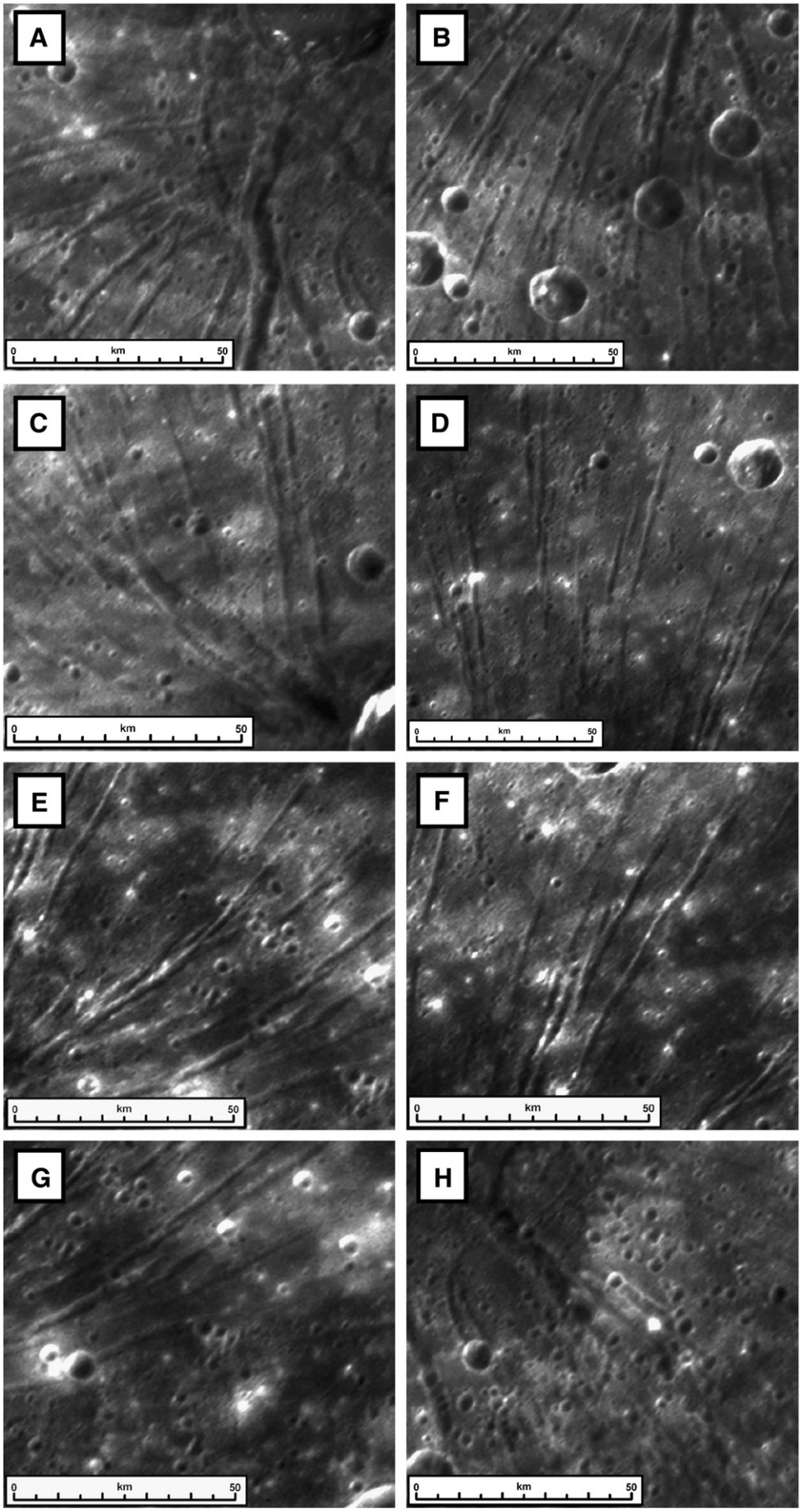
A
0 km 50
B
0 km 50
C
0 km 50
D
0 km 50
E
0 km 50
F
0 km 50
G
0 km 50
H
0 km 50

numerous examples of asymmetrical graben development apparently related to heterogeneous regional stress fields are also seen there (Grosfils and Head, 1994a,b). The lateral extent of the dense Pantheon Fossae plexus of radial graben (~175 km radius) is similar to typical novae on Venus (up to ~175 km radius) and well within the range of radial dikes and graben associated with central magma reservoirs on Earth, Mars, and Venus (up to several thousand kilometers) (Parfitt and Head, 1993; Grosfils and Head, 1994b; Ernst et al., 1995; Wilson and Head, 2002).

Initial analyses of Pantheon Fossae (Murchie et al., 2008; Head et al., 2008; Watters et al., 2009a,b-this issue) indicate that some of the radial graben extend well past the central plexus of graben and intersect a concentric deformation system of ridges and graben (Fig. 7B, C). Illumination conditions during MESSENGER's first Mercury flyby were not optimal for confident detection of all of the extended radial features, but fewer and longer graben in some sectors would be consistent with periodic buffered dike emplacement conditions (Parfitt and Head, 1993). Some of the radial graben systems on Venus have vents and lava flows associated with individual graben (Krassilnikov and Head, 2003) (Fig. 10). No similar flow-like features or small edifices have yet been observed associated with Pantheon Fossae, although the illumination geometry, resolution, and homogeneous color properties of the volcanic fill (Murchie et al., 2008; Robinson et al., 2008; Watters et al., 2009a,b-this issue) make any such detection difficult with existing data.

Additional characteristics of Pantheon Fossae graben that suggest that they are related to dikes include some *en echelon* patterns (suggesting rotation of dikes to accommodate shallow near-surface stress fields), cross-cutting relationships (suggesting successive dike emplacement events), and cuspate walls and some crater-chain-like structures (observed in dike-related graben due to collapse and gas venting).

The details of novae on Venus provide important information to assess Pantheon Fossae (Fig. 9). These features have been interpreted to represent doming and fracturing of the surface accompanied by radial dike emplacement that creates graben (Fig. 9A–C) and associated volcanic flows (Fig. 10) (Krassilnikov and Head, 2003; Grindrod et al., 2005). The process interpreted to be responsible is the upwelling of mantle material and associated thermal and dynamic uplift to create locally high topography and some radial fractures. The creation of a shallow magma reservoir during this period results in overpressurization events and radial dike emplacement to produce near-surface stress fields resulting in radial graben. Depending on the relationship of the depths of these dikes to the surface, they can create graben with no associated effusion (Fig. 9A) or can produce surface eruptions often along the graben or at their termini (Fig. 10) (Wilson and Head, 2006). In many cases, these structures are close enough to the surface to produce topographic highs, ring structures, or depressions (Fig. 9A–B (Krassilnikov and Head, 2003). If the Pantheon Fossae complex indeed represents a radial dike swarm, the lack of apparent concentric structures and the paucity of evidence for effusive flows in the available data suggest relatively greater depths for the reservoir than for many of the novae on Venus (Fig. 10). Indeed, the structure of Pantheon Fossae is very similar to the Venus nova shown in Fig. 9. This nova has radial symmetry, two length and width populations, some curved elements, cross-cutting graben, some *en echelon* segments, large cross-cutting graben in the nexus, and many graben that are exposed as a series of short segments. Dissimilarities include the topographic high associated with the Venus nova (Fig. 9B) and the low number of superposed impact craters. Currently available

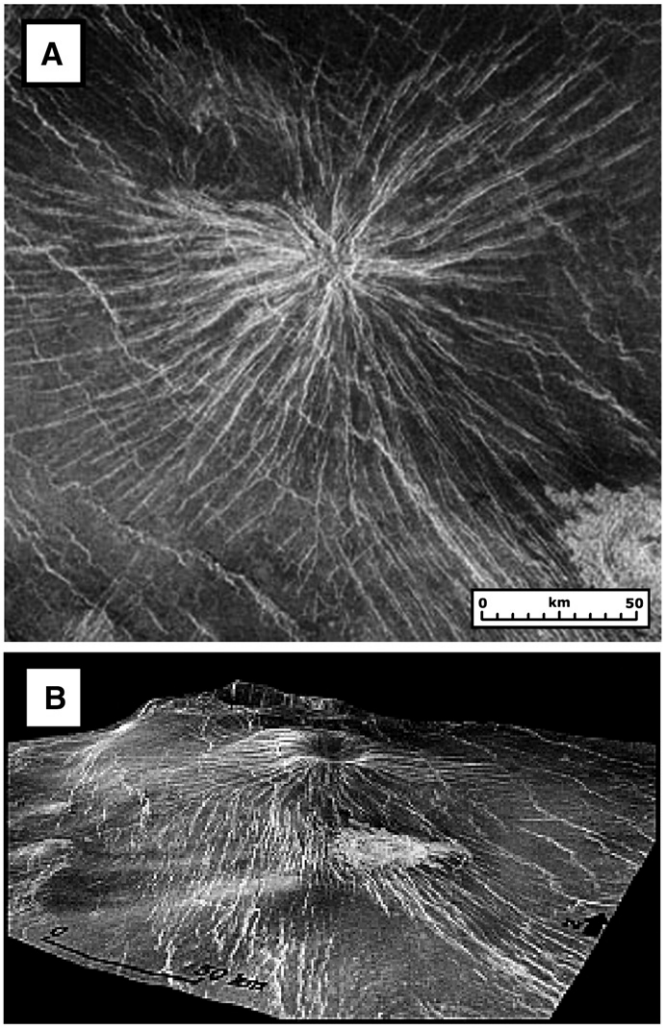

Fig. 9. Radial graben structures (novae) on Venus that are interpreted to be formed as radial dike swarms (e.g., Krassilnikov and Head, 2003). (A) Radar image of Becuma nova structure (34°N, 21.5°E), portion of Magellan image C1-MIDR 30N027.102. (B) Perspective view of radar image, looking north–northwest with 20× vertical exaggeration.

MESSENGER data do not permit the detection of any topography that might be associated with the nexus of Pantheon Fossae, and the superposition of Apollodorus crater further complicates the detection of any Pantheon topography. Altimetry data collected during the MESSENGER orbital mission will help to clarify these relationships.

The Pantheon Fossae complex is one of the few examples of extensional deformation yet seen on Mercury and the only radial graben structure observed thus far. The dominant global mode of deformation on Mercury is contractional, manifested in the form of tectonic ridges, scarps, and wrinkle ridges (Melosh and McKinnon, 1988; Solomon et al., 2008; Watters et al., 2009a,b-this issue), with the major exception being the concentric belt of graben inside the Caloris basin, observed in Mariner 10 data (Strom et al., 1975; Spudis and Guest, 1988; Melosh and McKinnon, 1988). A global contractional state of stress in the lithosphere is the product of a cooling interior (e.g., Solomon, 1977, 1978), which is also accompanied by a thickening

Fig. 8. Enlargements of portions of Pantheon Fossae, starting near the center (A), and then working generally clockwise from the south (B–H). Images and some of the characteristics of the radial graben swarm are described in more detail in the text. All images are subframes of MDIS NAC images. (A) EN0108826822M. (B) EN0108826822M. (C) EN0108826757M. (D) EN0108826757M. (E) EN0108826757M. (F) EN0108826757M. (G) EN0108826822M. (H) EN0108826822M.

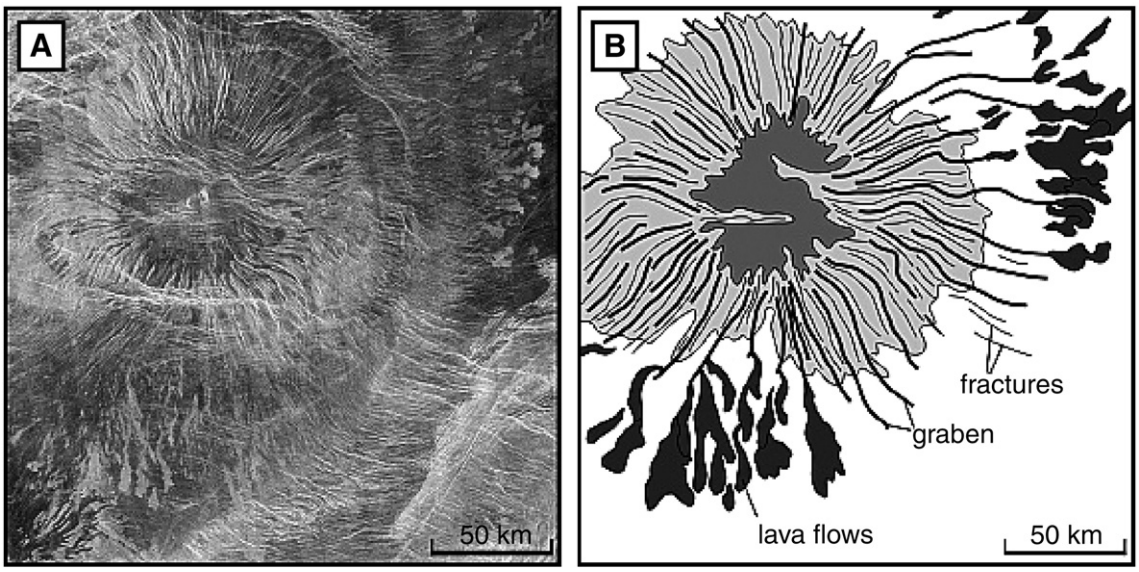

Fig. 10. Typical example of a nova (14°S, 164°E) showing radial structure of graben and fractures and related lava flows generally emanating from the ends of the graben. These types of relationships support the interpretation of many novae as surface manifestations of shallow dike emplacement events. (A) Portion of Magellan radar image C1-MIDR 15S163.101. (B) Sketch map. After Krassilnikov and Head (2003).

lithosphere, a decrease in the ability of mantle convective patterns to disrupt the lithosphere, a decrease in the amount of mantle partial melt, and a decrease in the ability of dikes to reach the surface (e.g., Head and Wilson, 1992). These general trends would decrease the likelihood of shallow magma reservoirs and associated radial dike swarms. In such a global tectonic environment, however, impact craters and basins can cause perturbations to both the stress state and the thermal structure. The formation of an impact feature relieves pre-existing stress within the crater and a more extensive zone of mechanical damage (e.g., Freed et al., 2009-this issue) and heats the interior through the conversion of impact kinetic energy to heat and uplift of isotherms during basin collapse (e.g., Bratt et al., 1985). A large basin may therefore provide an effective focus for mantle upwelling, melt generation, magma ascent, and near-surface extension (e.g., Elkins-Tanton et al., 2004; Ghods and Arkani-Hamed, 2007).

In summary, we find that the hypothesis of a magmatic origin for Pantheon Fossae is worthy of further investigation. Specific simulations of the development of such a feature should include the formation of the Caloris basin, the response of the crust and mantle to basin formation, the generation and ascent of magma, and the near-surface stress field though time, and particular attention should be paid to why the history of the Caloris basin has differed from basins of comparable size on the Moon and other terrestrial planets. Given the context of an overall model for Caloris, formation of a shallow magma reservoir would result in radial dike propagation; the symmetry of the dikes is consistent with formation in the center of a circular basin where stresses are most likely to be horizontally isotropic. Buffered and unbuffered reservoir conditions (Parfitt and Head, 1993) can plausibly account for the two radial ranges of graben. These predictions can be further tested with altimeter and gravity observations, high-resolution imaging, and searches for analogous features in previously unseen areas of Mercury.

5. Discussion and conclusions

The first MESSENGER flyby has confirmed Mariner 10 interpretations that volcanism was responsible for the formation of many occurrences of regional plains on Mercury (Strom et al., 1975; Robinson and Lucey, 1997). The view of the area imaged for the first time during the MESSENGER flyby (an additional 21% of the surface and the full Caloris basin interior) has served to underline the paucity of occurrences of extensional deformation that might reflect subsurface magmatic events. We describe three occurrences: (1) a floor-fractured crater on the margin of plains interpreted to be of volcanic origin (Head et al., 2008, 2009-this issue) that appears to be formed by shallow sill intrusion and laccolith formation; (2) a set of concentric graben inside the central peak ring of the ~250-km-diameter crater Raditladi (Prockter et al., 2008) that could be the surface expression of cone sheets and ring dikes, or alternatively of post-infill uplift of the central basin floor; (3) the Pantheon Fossae complex, a ~350-km-diameter radial graben swarm located in the center of the Caloris basin, which has been ascribed to several processes. We examine the similarity of this last feature to radial dike swarms known or interpreted on other planets and conclude that this hypothesis merits further testing as an origin for this structure. New data to be obtained by the MESSENGER and BepiColombo missions will be required to distinguish among the several hypotheses for Pantheon Fossae. Higher-resolution data taken at different solar illumination geometries will permit further documentation of its geometry and its relationship to Caloris basin fill, associated tectonic features, and Apollodorus crater. These data will enable us to address further the questions: What is the origin of the graben and are there any vent-related features and structures? Why are the graben so symmetrically arrayed? Why is the only known occurrence of such a structure in the center of the Caloris basin? Is the location of Apollodorus crater coincidental or genetically related to Pantheon Fossae?

The scarcity of extensional features on Mercury, and the location of those that are observed in impact basin interiors and adjacent to plains of volcanic origin, supports other observations of the tectonic and volcanic style of Mercury (Wilson and Head, 2008). The emerging picture of the volcanic style of Mercury is similar to that of the Moon, the other small one-plate planet (Wilson and Head, 2008): there are no major shield volcanoes, shallow magma reservoirs are rare, and there is little evidence of broadly distributed mantle upwelling associated with deformation of the surface or shallow volcanic sources. Because of the dominance of contractional deformation, evidence for shallow intrusions (e.g., dikes and sills) may be even rarer on Mercury than on the Moon, and such shallow intrusive events may require special circumstances (large crater or basin formation) to provide regional thermal and stress environments that deviate from the general global trend. These hypotheses can be further tested with new MESSENGER and BepiColombo data.

Acknowledgements

We gratefully acknowledge the personnel of the Johns Hopkins University Applied Physics Laboratory who have planned and executed the MESSENGER mission. Without their dedication and perseverance, this analysis would not have been possible. We gratefully acknowledge Kris Becker, Mark Robinson, Brett Denevi, and all those who have processed and calibrated the MDIS data. Thanks are extended to Wouter Bleeker and an unidentified reviewer whose careful reviews improved the quality of the paper. The MESSENGER project is supported by the NASA Discovery Program under contracts NASW-00002 to the Carnegie Institution of Washington and NAS5-97271 to the Johns Hopkins University Applied Physics Laboratory.

References

Anderson, E.M., 1936. The dynamics of the formation of cone-sheets, ring-dykes and caldron-subsidences. Proc. R. Soc. Edinb. 56, 128–156.
Banerdt, W.B., Golombek, M.P., Tanaka, K.L., 1992. Stress and tectonics on Mars. In: Kieffer, H.H., Jakosky, B.M., Snyder, C.W., Matthews, M.S. (Eds.), Mars. University of Arizona Press, Tucson, Ariz., pp. 249–297.
Basilevsky, A.T., Head, J.W., 2007. Beta Regio, Venus: evidence for uplift, rifting, and volcanism due to a mantle plume. Icarus 192, 167–186.
Benkhoff, J., Fujimoto, M., Laakso, H., in press. Science goals of BepiColombo. Planet. Space Sci.
Blake, S., 1981. Volcanism and the dynamics of open magma chambers. Nature 289, 783–785.
Bleeker, W., 2002. Archean tectonics: a review, with illustrations from the Slave Craton. In: Fowler, C.M.R., Ebinger, C.J., Hawkesworth, C.J. (Eds.), The Early Earth: Physical, Chemical and Biological Development. Special Publication, vol. 199. Geological Society, London, pp. 151–181.
Bleeker, W., 2003. The late Archean record: a puzzle in ca. 35 pieces. Lithos 71, 99–134.
Bleeker, W., 2004. Taking the pulse of planet Earth: a proposal for a new multi-disciplinary flagship project in Canadian solid Earth sciences. Geosci. Can. 31, 179–190.
Bleeker, W., Ernst, R.E., 2006. Short-lived mantle generated magmatic events and their dyke swarms: the key unlocking Earth's paleogeographic record back to 2.6 Ga. In: Hanski, E., Mertanen, S., Rämö, T., Vuollo, J. (Eds.), Dyke Swarms — Time Markers of Crustal Evolution. Taylor & Francis, London, pp. 3–26.
Blewett, D.T., Robinson, M.S., Denevi, B.W., Gillis-David, J.J., Head, J.W., Solomon, S.C., Holsclaw, G.M., McClintock, W.E., 2009. Multispectral imaging of Mercury from the first MESSENGER flyby: analysis of global and regional color trends. Earth Planet. Sci. Lett. 285, 272–282 (this issue).
Bratt, S.R., Solomon, S.C., Head, J.W., 1985. The evolution of impact basins: cooling, subsidence, and thermal stress. J. Geophys. Res. 90, 12415–12433.
Carr, M.H., 2006. Water on Mars. Oxford University Press, New York. 229 pp.
Crumpler, L.S., Aubele, J.C., 2000. Volcanism on Venus. In: Sigurdsson, H. (Ed.), Encyclopedia of Volcanoes. Academic Press, San Diego, Calif., pp. 727–770.
Delaney, P.T., 1987. Heat transfer during emplacement and cooling of mafic dykes. In: Halls, H.C., Fahrig, W.F. (Eds.), Mafic Dyke Swarms. Special Paper, vol. 34. Geological Society of Canada, pp. 34–46.
Delaney, P.T., Pollard, D.D., 1981. Deformation of host rocks and flow of magma during growth of minette dikes and breccia bearing intrusions near Ship Rock, New Mexico. Professional Paper 1202. U.S. Geological Survey, Denver, Colo. 61 pp.
Dombard, A.J., Gillis, J.J., 2001. Testing the viability of topographic relaxation as a mechanism for the formation of lunar floor-fractured craters. J. Geophys. Res. 106, 27901–27910.
Elkins-Tanton, L.T., Hager, B.H., Grove, T.L., 2004. Magmatic effects of the lunar late heavy bombardment. Earth Planet. Sci. Lett. 222, 17–27.
Ernst, R.E., Baragar, W.R.A., 1992. Evidence from magnetic fabric for the flow pattern of magma in the Mackenzie giant radiating dyke swarm. Nature 356, 511–513.
Ernst, R.E., Head, J.W., Parfitt, E., Grosfils, E., Wilson, L., 1995. Giant radiating dike swarms on Earth and Venus. Earth Sci. Rev. 39, 1–58.
Ernst, R.E., Desnoyers, D.W., Head, J.W., Grosfils, E.B., 2003. Graben–fissure systems in Guinevere Planitia and Beta Regio (264–312°E, 24–60°N), Venus, and implications for regional stratigraphy and mantle plumes. Icarus 164, 282–316.
Fornari, D.J., 1987. The geomorphic and structural development of Hawaiian submarine rift zones. In: Decker, R.W., Wright, T.L., Stauffer, P.H. (Eds.), Volcanism in Hawaii. Professional Paper 1350, vol. 1. U.S. Geological Survey, Denver, Colo., pp. 125–132.
Freed, A.M., Solomon, S.C., Watters, T.R., Phillips, R.J., Zuber, M.T., 2009. Could Pantheon Fossae be the result of the Apollodorus crater-forming impact within the Caloris basin, Mercury? Earth Planet. Sci. Lett. 285, 320–327 (this issue).
Ghods, A., Arkani-Hamed, J., 2007. Impact-induced convection as the main mechanism for formation of lunar mare basalts. J. Geophys. Res. 112, E03005. doi:10.1029/2006JE002709.
Gillis-Davis, J., Blewett, D.T., Gaskell, R.W., Denevi, B.W., Robinson, M.S., Strom, R.G., Solomon, S.C., Sprague, A.L., 2009. Pit-floor craters on Mercury: evidence of near-surface igneous activity. Earth Planet. Sci. Lett. 285, 243–250 (this issue).
Grindrod, P.M., Nimmo, F., Stofan, E.R., Guest, J.E., 2005. Strain at radially fractured centers on Venus. J. Geophys. Res. 110, E12002. doi:10.1029/2005JE002416.
Grosfils, E.B., 2007. Magma reservoir failure on the terrestrial planets: assessing the importance of gravitational loading in simple elastic models. J. Volcan. Geotherm. Res. 166, 47–75.
Grosfils, E.B., Head, J.W., 1994a. The global distribution of giant radiating dike swarms on Venus: implications for the global stress state. Geophys. Res. Lett. 21, 701–704.
Grosfils, E.B., Head, J.W., 1994b. Emplacement of a radial dike swarm in Vinmara Planitia, Venus: interpretation of the regional stress field orientation and subsurface magmatic configuration. Earth Moon, Planets 66, 153–171.
Gudmundsson, A., 1984. Formation of dykes, feeder-dykes, and the intrusion of dykes from magma chambers. Bull. Volcanol. 47, 537–550.
Hall, J.L., Solomon, S.C., Head, J.W., 1981. Lunar floor-fractured craters: evidence for viscous relaxation of crater topography. J. Geophys. Res. 86, 9537–9552.
Halls, H.C., 1982. The importance and potential of mafic dyke swarms in studies of geodynamic processes. Geosci. Can. 9, 145–154.
Head, J.W., Wilson, L., 1979. Alphonsus-type dark-halo craters: morphology, morphometry, and eruption conditions. Proc. Lunar Planet. Sci. Conf. 10, 2861–2897.
Head, J.W., Wilson, L., 1991. Absence of large shield volcanoes and calderas on the Moon — consequence of magma transport phenomena? Geophys. Res. Lett. 18, 2121–2124.
Head, J.W., Wilson, L., 1992. Lunar mare volcanism: stratigraphy, eruption conditions, and the evolution of secondary crusts. Geochim. Cosmochim. Acta 55, 2155–2175.
Head, J.W., Wilson, L., 1993. Lunar graben formation due to near-surface deformation accompanying dike emplacement. Planet. Space Sci. 41, 719–727.
Head, J.W., Crumpler, L.S., Aubele, J.C., Guest, J.E., Saunders, R.S., 1992. Venus volcanism: classification of volcanic features and structures, associations, and global distribution from Magellan data. J. Geophys. Res. 97, 13153–13197.
Head, J.W., Murchie, S.L., Prockter, L.M., Robinson, M.S., Solomon, S.C., Strom, R.G., Chapman, C.R., Watters, T.R., McClintock, W.E., Blewett, D.T., Gillis-Davis, J.J., 2008. Volcanism on Mercury: evidence from the first MESSENGER flyby. Science 321, 69–72.
Head, J.W., Murchie, S.L., Prockter, L.M., Solomon, S.C., Chapman, C.R., Strom, R.G., Watters, T.R., Blewett, D.T., Gillis-Davis, J.J., Fassett, C.I., Dickson, J.L., Morgan, G.A., Kerber, L., 2009. Volcanism on Mercury: evidence from the first MESSENGER flyby for extrusive and explosive activity and the volcanic origin of plains. Earth Planet. Sci. Lett. 285, 227–242 (this issue).
Holcomb, R.T., 1987. Eruptive history and long-term behavior of Kilauea Volcano. In: Decker, R.W., Wright, T.L., Stauffer, P.H. (Eds.), Volcanism in Hawaii. Professional Paper 1350, vol. 1. U.S. Geological Survey, Denver, Colo., pp. 261–350.
Johnson, R.B., 1961. Patterns and origins of radial dike swarms associated with West Spanish Peak and Dike Mountain, south-central Colorado. Geol. Soc. Am. Bull. 72, 579–589.
Kerber, L., Head, J.W., Solomon, S.C., Murchie, S.L., Blewett, D.T., Wilson, L., 2009. Explosive volcanic eruptions on Mercury: eruption conditions, magma volatile content, and implications for mantle volatile abundances. Earth Planet. Sci. Lett. 285, 263–271 (this issue).
Krassilnikov, A.S., Head, J.W., 2003. Novae on Venus: geology, classification, and evolution. J. Geophys. Res. 108 (5108). doi:10.1029/2002JE001983.
Le Bas, M.J., 1971. Cone-sheets as a mechanism of uplift. Geol. Mag. 108, 373–376.
Mastin, L.G., Pollard, D.D., 1988. Surface deformation and shallow dike intrusion processes at Inyo Craters, Long Valley, California. J. Geophys. Res. 93, 13221–13235.
Melosh, H.J., McKinnon, W.B., 1988. The tectonics of Mercury. In: Vilas, F., Chapman, C.R., Matthews, M.S. (Eds.), Mercury. University of Arizona Press, Tucson, Ariz., pp. 374–400.
Murchie, S., Watters, T.R., Robinson, M.S., Head, J.W., Strom, R.G., Chapman, C.R., Solomon, S.C., McClintock, W.E., Prockter, L.M., Domingue, D.L., Blewett, D.T., 2008. Geology of the Caloris basin, Mercury: a view from MESSENGER. Science 321, 73–76.
Odé, H., 1957. Mechanical analysis of the dike pattern of the Spanish Peaks area, Colorado. Geol. Soc. Am. Bull. 68, 567–576.
Parfitt, E.A., 1991. The role of rift zone storage in controlling the site and timing of eruptions and intrusions at Kilauea volcano, Hawaii. J. Geophys. Res. 96, 10101–10112.
Parfitt, E.A., Head, J.W., 1993. Buffered and unbuffered dike emplacement on Earth and Venus: implications for magma reservoir size, depth, and rate of magma replenishment. Earth Moon Planets 61, 249–281.
Parker, A.J., Rickwood, P.C., Tucker, D.H. (Eds.), 1990. Mafic Dykes and Emplacement Mechanisms. Balkema, Rotterdam, 541 pp.
Phillips, W.J., 1974. The dynamic emplacement of cone-sheets. Tectonophysics 24, 69–84.
Pike, R.J., 1980. Geometric interpretation of lunar craters. Professional Paper 1046-C. U.S. Geological Survey, Denver, Colo., pp. C1–C77.
Pike, R.J., 1988. Geomorphology of impact craters on Mercury. In: Vilas, F., Chapman, C.R., Matthews, M.S. (Eds.), Mercury. University of Arizona Press, Tucson, Ariz., pp. 165–273.
Pollard, D.D., 1987. Elementary fracture mechanics applied to the structural interpretation of dykes. In: Halls, H.C., Fahrig, W.F. (Eds.), Mafic Dyke Swarms. Special Paper, vol. 34. Geological Association of Canada, pp. 5–24.
Pollard, D.D., Muller, O.H., 1976. The effect of gradients in regional stress and magma pressure on the form of sheet intrusions in cross section. J. Geophys. Res. 81, 975–984.
Pollard, D.D., Delaney, P.T., Duffield, W.A., Endo, E.T., Okamura, A.T., 1983. Surface deformation in volcanic rift zones. Tectonophysics 94, 541–584.
Prockter, L.M., Chapman, C.R., Gaskell, R.W., Solomon, S.C., Murchie, S.L., Barnouin-Jha, O.S., Robinson, M.S., Blewett, D.T., Watters, T.R., Head III, J.W., Gillis-Davis, J.J., 2008. Geology of the unusual double-ring Raditladi basin on Mercury. Eos Trans. AGU 89 (53), Fall Meeting suppl., abstract U21A-0020.
Robinson, M.S., Lucey, P.G., 1997. Recalibrated Mariner 10 color mosaics: implications for mercurian volcanism. Science 275, 197–200.
Robinson, M.A., Murchie, S.L., Blewett, D.T., Domingue, D.L., Hawkins, S.E., Head, J.W., Holsclaw, G.M., McClintock, W.E., McCoy, T.J., McNutt, R.L., Prockter, L.M., Solomon, S.C., Watters, T.R., 2008. Reflectance and color variations on Mercury: indicators of regolith processes and compositional heterogeneity. Science 321, 66–69.
Rubin, A.M., 1992. Dike-induced faulting and graben subsidence in volcanic rift zones. J. Geophys. Res. 97, 1839–1858.

Rubin, A.M., Pollard, D.D., 1987. Origins of blade-like dikes in volcanic rift zones. In: Decker, R.W., Wright, T.L., Stauffer, P.H. (Eds.), Volcanism in Hawaii. Professional Paper 1350, vol. 2. U.S. Geological Survey, Denver, Colo., pp. 1449–1470.
Ryan, M.P., 1988. The mechanics and three-dimensional internal structure of active magmatic systems: Kilauea volcano, Hawaii. J. Geophys. Res. 93, 4213–4248.
Schirnick, C., van den Bogaard, P., Schmincke, H.-U., 1999. Cone sheet formation and intrusive growth of an oceanic island — the Miocene Tejeda complex on Gran Canaria (Canary Islands). Geology 27, 207–210.
Schultz, P.H., 1976. Floor-fractured lunar craters. Moon 15, 241–273.
Schultz, P.H., 1977. Endogenic modification of impact craters on Mercury. Phys. Earth Planet. Inter. 15, 202–219.
Sigurdssson, H., 1987. Dyke injection in Iceland: a review. In: Halls, H.C., Fahrig, W.F. (Eds.), Mafic Dyke Swarms. Special Paper, vol. 34. Geological Association of Canada, pp. 55–64.
Solomon, S.C., 1977. The relationship between crustal tectonics and internal evolution in the Moon and Mercury. Phys. Earth Planet. Inter. 15, 135–145.
Solomon, S.C., 1978. On volcanism and thermal tectonics on one-plate planets. Geophys. Res. Lett. 5, 461–464.
Solomon, S.C., McNutt Jr., R.L., Watters, T.R., Lawrence, D.J., Feldman, W.C., Head, J.W., Krimigis, S.M., Murchie, S.L., Phillips, R.J., Slavin, J.A., Zuber, M.T., 2008. Return to Mercury: a global perspective on MESSENGER's first Mercury flyby. Science 321, 59–62.
Spudis, P.D., Guest, J.E., 1988. Stratigraphy and geologic history of Mercury. In: Vilas, F., Chapman, C.R., Matthews, M.S. (Eds.), Mercury. University of Arizona Press, Tucson, Ariz., pp. 118–164.
Strom, R.G., Trask, N.J., Guest, J.E., 1975. Tectonism and volcanism on Mercury. J. Geophys. Res. 80, 2478–2507.
Strom, R.G., Chapman, C.R., Merline, W.J., Solomon, S.C., Head, J.W., 2008. Mercury cratering record viewed from MESSENGER's first flyby. Science 321, 79–81.
Watters, T.R., Murchie, S.L., Robinson, M.S., Solomon, S.C., Denevi, B.W., André, S.L., Head, J.W., 2009a. Emplacement and tectonic deformation of smooth plains in the Caloris basin, Mercury. Earth Planet. Sci. Lett. 285, 309–319 (this issue).
Watters, T.R., Solomon, S.C., Robinson, M.S., Head, J.W., André, S.L., Hauck II, S.A., Head, J.W., 2009b. The tectonics of Mercury: the view after MESSENGER's first flyby. Earth Planet. Sci. Lett. 285, 283–296 (this issue).
Wichman, R.W., Schultz, P.H., 1996. Crater-centered laccoliths on the Moon: modeling intrusion depth and magmatic pressure at the crater Taruntius. Icarus 122, 193–199.
Wilson, L., Head, J.W., 2002. Tharsis-radial graben systems as the surface manifestation of plume-related dike intrusion complexes: models and implications. J. Geophys. Res. 107, 5057. doi:10.1029/2001JE001593.
Wilson, L., Head, J.W., 2006. Lateral dike injection and magma eruption around novae and coronae on Venus. Lunar Planet. Sci. 38 abstract 1125.
Wilson, L., Head, J.W., 2008. Volcanism on Mercury: a new model for the history of magma ascent and eruption. Geophys. Res. Lett. 35, L23205. doi:10.1029/2008GL035620.